A vibrational analysis of crystalline trans-1,4-polybutadiene

S. L. Hsu, W. H. Moore, and S. Krimm

Harrison M. Randall Laboratory of Physics, and Macromolecular Research Center, University of Michigan, Ann Arbor, Michigan 48104

The normal vibrations of crystalline trans-1,4-polybutadiene have been calculated by combining interchain atom-atom potentials with the previously proposed intrachain force field. These calculations have been used to analyze the infrared and Raman spectra of an essentially all-trans urea-complex polymer. The band splittings and low-frequency lattice modes observed in these spectra are satisfactorily accounted for by the calculations.

PACS numbers: 35.20.P, 78.30.J

INTRODUCTION

The structure of crystalline trans-1, 4-polybutadiene (TPBD) has been the subject of several x-ray diffraction studies.[1-3] These have formed the basis for a normal vibration analysis of the single TPBD chain.[4] This analysis has been used to interpret the infrared and Raman spectra of crystalline and noncrystalline TPBD structures,[5-8] the latter having particular relevance to the conformations in fold regions of TPBD single crystals.

The vibrational spectrum of TPBD exhibits, however, explicit evidence of interchain interactions, both in the splittings of intramolecular modes as well as in the observation (which we report here) of lattice modes associated with the crystalline regions. It is, therefore, clear that such interchain interaction effects must be satisfactorily taken into account before the spectrum can be used for relatively unambiguous assignments of bands of noncrystalline conformations.

In this paper we undertake a vibrational analysis of crystalline TPBD by adding interchain potential terms to the intramolecular force field previously used.[4] Our study is also more definitive in that we have obtained infrared and Raman data on a sample polymerized in urea complex, which is known,[9,10] and which we have confirmed to have essentially 100% trans units. By studying this TPBD in the as-polymerized state, which is highly crystalline, as well as in the form of single crystals, in which chain-folded conformations are present, we have also been able to better identify spectral features associated with the ordered and disordered chain conformations.

EXPERIMENTAL

The TPBD sample used in our studies was polymerized in urea complex by γ radiation and shows no evidence of cis groups. A small amount of vinyl groups may be present, as indicated by a very weak band at 1639 cm^{-1}.

Spectra were obtained on the above as-polymerized sample, as well as on single crystals. These were grown in 0.02% solutions of heptane, benzene, and xylene.[11] Probably because of the high molecular weight and regularity of this polymer, the minimum dissolution temperature, even in the best solvent (namely, benzene) was 62 °C, somewhat higher than reported previously. The Raman spectra of single crystals grown in heptane and xylene showed high backgrounds in the 0–200-cm^{-1} region, although at low temperatures the spectra of all samples were the same in this region. Annealed single crystals were prepared by heating *in vacuo* for 1 h at 96 °C.

Infrared spectra were obtained on a Perkin-Elmer Model 180 spectrophotometer and are similar to those published previously.[12] The far-infrared region was studied with a Digilab FTS-16 fourier transform spectrometer.

Raman spectra were obtained on a spectrometer built in our laboratory, incorporating a Spex 1400 monochromator, a Coherent Radiation 52G argon ion laser, and an ITT photomultiplier tube operating at −30 °C with standard photon counting techniques. The laser was generally operated at the 5145-Å line, although in the low-frequency studies, where an iodine absorption cell was used, the laser was single moded to the 5145.42-Å rotational line of iodine. Holographically ruled gratings with 1800 grooves/mm were used in the monochromator, which helped significantly in rejecting the Rayleigh scattering as compared to conventionally ruled gratings. Spectra presented in this paper were obtained with zero suppression.

A sample holder was designed to permit Raman (as well as infrared) spectra to be obtained between liquid-nitrogen temperature and 110 °C. A zero crossing proportional temperature controller (RCA 3059) enabled the temperature to be controlled to within 1 °C. In order to avoid oxidation, all Raman spectra were run in vacuo. In all cases, the spectra were obtained by the front-scattering technique.

Raman spectra of the as-polymerized TPBD at room temperature and 110 °K are shown in Figs. 1 and 2, respectively. Spectra of single crystals are shown in Figs. 3 (before annealing) and 4 (after annealing). Spectra in the low-frequency region at room temperature are shown in Fig. 5 (obtained on a Jobin Yvon Ramanor II spectrometer) and at 110 °K in Fig. 6.

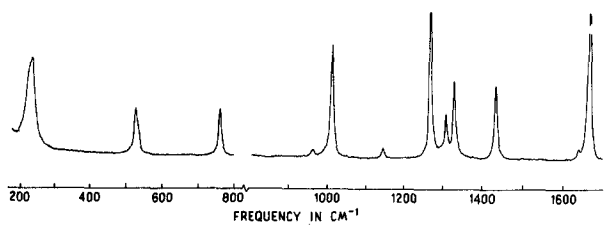

FIG. 1. Raman spectrum of TPBD at room temperature. Band pass, 2 cm^{-1} at 5100 Å. Laser power, 200 mW at 5145 Å.

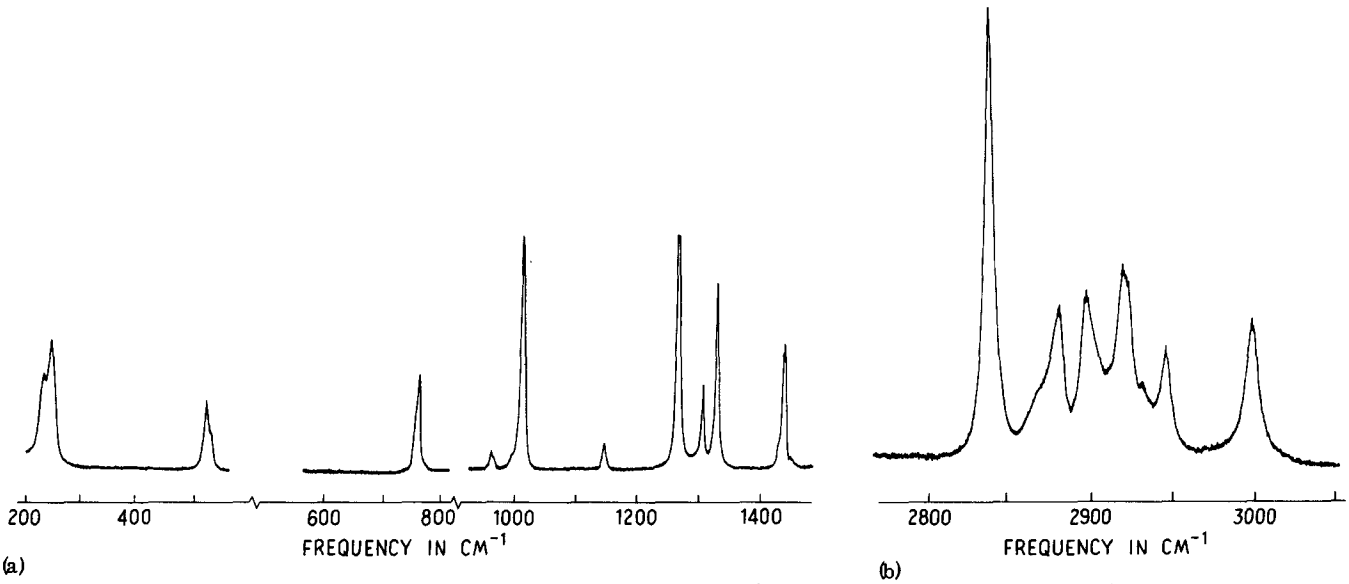

FIG. 2. Raman spectrum of TPBD at 110°K. Band pass, 2 cm^{-1} at 5100 Å. Laser power, 200 mW at 5145 Å. (a) 200—1400-cm^{-1} region; (b) 2800—3100-cm^{-1} region.

NORMAL VIBRATION CALCULATIONS

Structure and symmetry

The structure of the single chain of crystalline TPBD has been derived from x-ray diffraction studies.[1-3] It is agreed that in such a chain, represented in Fig. 7, the CH_2 groups are trans to each other, but there has not been agreement on the value of the =CH-CH_2- torsion angle φ. The structural parameters for the four proposed geometries are given in Table I. In all cases, however, the single chain has C_i symmetry (with the center of inversion at the center of the double bond). There are 14 Raman active A_g vibrations and 12 (mutually exclusive) infrared active A_u vibrations. The definitions of the internal coordinates used in the calculations are given in Table II, and those of the local symmetry coordinates are given in Table III.

The crystal structure proposed by Iwayanagi *et al.*[2] consists of four molecules in a monoclinic unit cell with space group $P2_1/a$. The unit cell, projected along the c (fiber) axis, is shown in Fig. 8. The coordinates of the center of the double bond are $X=\frac{1}{4}$, $Y=\frac{1}{8}$, and $Z=\frac{1}{4}$. The setting angle, defined as the angle between the C_1-C_4 bond and the $a\sin\beta$ axis, is taken to be 120°, and the interchain separation is 4.54 Å. The space group $P2_1/a$ corresponds to the factor group C_{2h}, with Raman active A_g and B_g species and infrared active A_u and B_u species. The following numbers of internal vibrational, lattice translatory, and lattice rotatory modes are associated with each of the symmetry species: A_g—26, 3, and 1; B_g—26, 3, and 1; A_u—26, 2, and 1; B_u—26, 1, and 1.

It should be noted that the inversion center in the crystal is no longer at the center of the -CH=CH- bond but is now between chains. This means that, strictly speaking, the mutual exclusion principle should no longer apply to the single-chain modes. However, since the perturbation of the intrachain potential by the interchain interactions is very small except in those cases where H···H interactions make a significant contribution, we expect the mutual exclusion principle to apply within a good approximation except for intrachain modes involving large contributions from H motions.

Force fields

The intrachain potential function for TPBD has been taken from the work of Neto and di Lauro.[4] The only change we have made is to take $H_\Gamma=2.999$ rather than 1.999 as given in their paper. This force constant affects only the C=C torsion and C-H out-of-plane modes (both of which are relatively pure modes), and the lower number (which we believe to be in error) gives rise to predicted frequencies which are about 125 cm^{-1} lower than the (unambiguously assigned) observed bands.

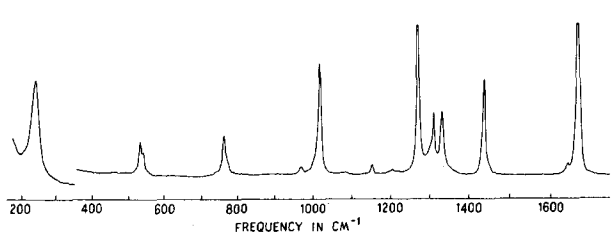

FIG. 3. Raman spectrum of TPBD single crystals before annealing, at room temperature. Band pass, 1.5 cm^{-1} at 5100 Å. Laser pwer, 300 mW at 5145 Å.

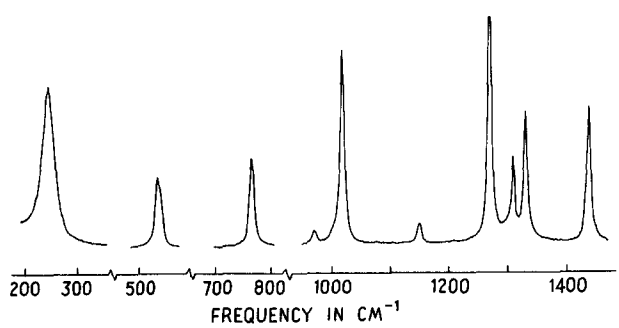

FIG. 4. Raman spectrum of TPBD single crystals after annealing, at room temperature. Band pass, <1 cm^{-1} at 5100 Å. Laser power, 300 mW at 5145 Å.

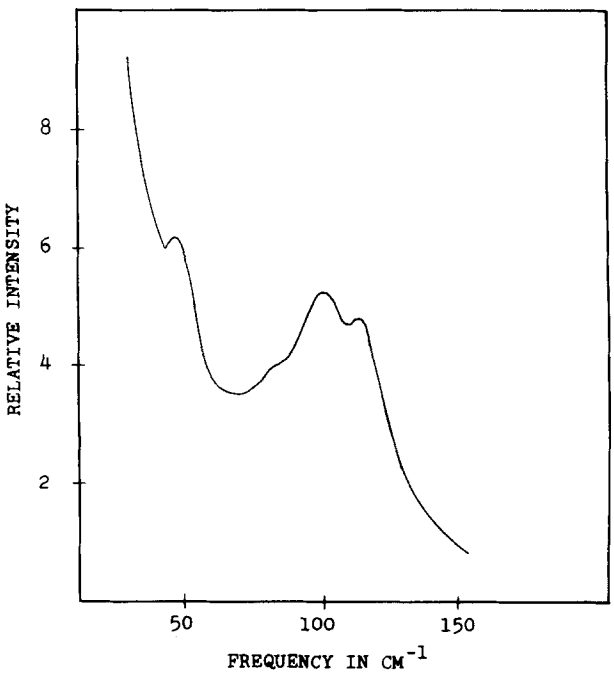

FIG. 5. Low-frequency Raman spectrum of TPBD at room temperature (obtained on a Jobin Yvon Ramanor II spectrometer). Band pass, < 3 cm^{-1}. Laser power, 300 mW at 5145 Å.

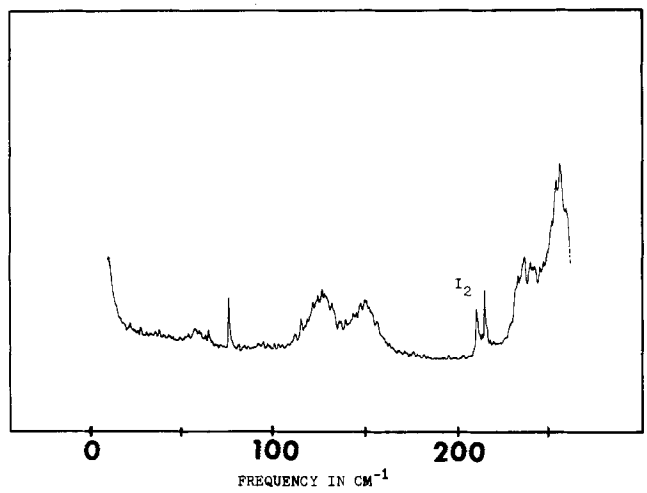

FIG. 6. Low-frequency Raman spectrum of TPBD at 110°K, using an iodine absorption cell. Band pass, 3 cm^{-1}. Laser power, 150 mW at 5145.42 Å.

The interchain potential is comprised of atom-atom interactions, in particular the set IV potentials of Williams.[13] These potentials are of the form $Ad^{-6} + B\exp(-Cd)$, where d is the interatomic distance. The constants are as follows: for H···H: $A = -27.3$ kcal/mole Å^6, $B = 2654$ kcal/mole, and $C = 3.74$ Å^{-1}; for C···H: $A = -125$, $B = 8766$, and $C = 3.67$; and for C···C: $A = -568$, $B = 83,630$, and $C = 3.60$. The attraction-repulsion center for the H atom was assumed to be located 0.07 Å toward the C atom along the C-H bond.[14] We have used radii of interaction of 3.5, 4.0, and 4.3 Å for the H···H, C···H, and C···C interactions, respectively. Force constants were obtained by double differentiation of the potential, with first derivative terms included in their evaluation.

Normal vibration frequencies

An analysis of the vibrational spectrum of TPBD, and of its changes with temperature and sample preparation, requires that we understand the effect of intermolecular interactions on the frequencies of a single chain. It is also necessary, however, to consider the possibility that changes in chain conformation may occur under these conditions, and such structural changes could also affect the spectrum. In order to determine the sensitivity of the vibrational frequencies to conformational changes in the crystal, we have calculated the normal vibrations of a single chain for various values of φ, corresponding to the different crystalline chain conformations suggested in the literature. These conformations are within the range of low-energy structures determined from conformational energy analysis.[15] The results are presented in Table IV. It will be seen that some of the modes, in particular, the lower-frequency Raman-active vibrations, are especially sensitive to changes in φ. Since these modes involve skeletal defor-

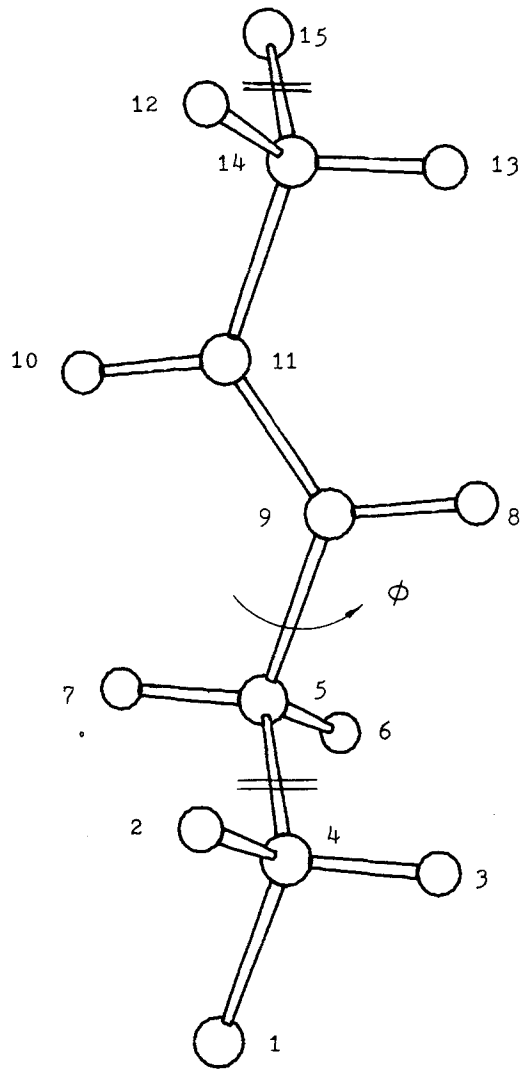

Trans 1-4 Polybutadiene

FIG. 7. Single chain of TPBD. Atoms numbered in accordance with definition of internal coordinates.

TABLE I. Structural parameters of proposed geometries of a single chain of trans-1, 4-polybutadiene.

	A[a]	B[b]	C[c]	D[d]
l(=C-H) (Å)	1.09	1.09	1.09	1.09
l(-C-H) (Å)	1.10	1.10	1.10	1.10
l(-C=C-) (Å)	1.34	1.34	1.34	1.34
l(=C-C-) (Å)	1.52	1.54	1.54	1.54
l(-C-C-) (Å)	1.52	1.54	1.54	1.54
< (-C-C=C-) (deg)	125	125	125	125
< (-C-C-C-) (deg)	110	109.5	109.5	109.5
< (H-C-H) (deg)	109.5	109.5	109.5	109.5
τ(=C-C-) (deg)	60	60	71	100
τ(-C-C-) (deg)	0	0	0	0
Repeat (Å)	4.85	4.89	4.83	4.66

[a]Neto and di Lauro (Ref. 4).
[b]Natta and Corradini (Ref. 1).
[c]Iwayanagi, *et al.* (Ref. 2).
[d]High-temperature form (Ref. 3).

mations, and since the specific frequencies are sensitive to the equilibrium values of the chain angles, the trends in the frequency shifts are probably more reliable at this stage than the shifts themselves. Furthermore, since the calculation involved only changes in geometry, and since, in particular, certain internal interaction force constants are likely to be sensitive to the value of φ, it is probable that true frequency shifts with φ are not properly reproduced by this calculation in the region above about 1000 cm^{-1}. Nevertheless, the results in Table IV are useful in assessing the relative effects of conformational changes on specific normal modes.

The normal vibration frequencies of crystalline TPBD are given in Tables V and VI. The calculation is for chains with $\varphi = 60°$ in the unit cell of Iwayanagi *et al.*[2] The observed Raman and infrared bands are also given in these tables, and their assignments are discussed below.

DISCUSSION

Spectra

As noted earlier, our sample of TPBD is comprised almost 100% of trans units and, because of its high crystallinity, is undoubtedly dominated by essentially one-chain conformation. Since it may, however, contain some disordered material,[10] we must be cognizant of bands which may be due to other than the major crystalline conformation. The single-crystal spectra are helpful in this connection, since our present as well as earlier[6,8,16] results clearly indicate that the amount of noncrystalline component decreases after annealing. Thus, as can be seen from Figs. 3 and 4, annealing results in the disappearance of some bands (at 1202 and 1078 cm^{-1}) and the "sharpening" of others (near 760 and 530 cm^{-1}), as well as a change in I(1331)/I(1310), from 1.0 to 1.6, which is consistent with the improvement in order that takes place in the as-polymerized TPBD when the temperature is lowered (compare Figs. 1 and 2). These results suggest, therefore, that the band at 539 cm^{-1} (and perhaps one at 970 cm^{-1}) in the

TABLE III. Definitions of local symmetry coordinates.

C-C(R) str	$S_1 = R_1$
C-C(T) str	$S_2 = R_2$
C=C(D) str	$S_3 = R_3$
C-C(T) str	$S_4 = R_4$
CH sym str	$S_5 = (R_5 + R_6)/2^{1/2}$
CH asy str	$S_6 = (R_5 - R_6)/2^{1/2}$
=C-H	$S_7 = R_7$
=C-H	$S_8 = R_8$
CH sym str	$S_9 = (R_9 + R_{10})/2^{1/2}$
CH asy str	$S_{10} = (R_9 - R_{10})/2^{1/2}$
CH_2 wag	$S_{11} = (R_{11} + R_{12} - R_{14} - R_{15})/2$
CH_2 bend	$S_{12} = (4R_{13} - R_{11} - R_{12} - R_{14} - R_{15})/20^{1/2}$
CH_2 twist	$S_{13} = (R_{11} - R_{12} - R_{14} + R_{15})/2$
CH_2 rock	$S_{14} = (R_{11} - R_{12} + R_{14} - R_{15})/2$
CCC def	$S_{15} = (5R_{16} - R_{11} - R_{12} - R_{13} - R_{14} - R_{15})/30^{1/2}$
CCC′ def	$S_{16} = (2R_{18} - R_{17} - R_{19})/6^{1/2}$
CH ipb	$S_{17} = (R_{17} - R_{19})/2^{1/2}$
CCC′ def	$S_{18} = (2R_{21} - R_{20} - R_{22})/6^{1/2}$
CH ipb	$S_{19} = (R_{20} - R_{22})/2^{1/2}$
CH_2 wag	$S_{20} = (R_{24} + R_{25} - R_{27} - R_{28})/2$
CH_2 bend	$S_{21} = (4R_{26} - R_{24} - R_{25} - R_{27} - R_{28})/20^{1/2}$
CH_2 twist	$S_{22} = (R_{24} - R_{25} - R_{27} - R_{28})/2$
CH_2 rock	$S_{23} = (R_{24} - R_{25} + R_{27} - R_{28})/2$
CCC def	$S_{24} = (5R_{23} - R_{24} - R_{25} - R_{26} - R_{27} - R_{28})/30^{1/2}$
CH opb	$S_{25} = R_{29}$
CH opb	$S_{26} = R_{30}$
C-C(R) tor	$S_{27} = R_{31}$
C-C(T) tor	$S_{28} = R_{32}$
C=C tor	$S_{29} = R_{33}$
C-C(T) tor	$S_{30} = R_{34}$

TABLE II. Definitions of internal coordinates.

	Atoms		Atoms
$R_1 = r$(C-C)	(4,5)	$R_{18} =$ < (CCC)	(5,9,11)
$R_2 = r$(C-C)	(5,9)	$R_{19} =$ < (CCH)	(11,9,8)
$R_3 = r$(C=C)	(9,11)	$R_{20} =$ < (CCH)	(9,11,10)
$R_4 = r$(C-C)	(11,14)	$R_{21} =$ < (CCC)	(9,11,14)
$R_5 = r$(C-H)	(14,12)	$R_{22} =$ < (CCH)	(14,11,10)
$R_6 = r$(C-H)	(14,13)	$R_{23} =$ < (CCC)	(11,14,15)
$R_7 = r$(C-H)	(11,10)	$R_{24} =$ < (CCH)	(11,14,12)
$R_8 = r$(C-H)	(9,8)	$R_{25} =$ < (CCH)	(11,14,13)
$R_9 = r$(C-H)	(5,7)	$R_{26} =$ < (HCH)	(12,14,13)
$R_{10} = r$(C-H)	(5,6)	$R_{27} =$ < (CCH)	(15,14,12)
$R_{11} =$ < (CCH)	(4,5,6)	$R_{28} =$ < (CCH)	(15,14,13)
$R_{12} =$ < (CCH)	(4,5,7)	$R_{29} =$ CH opb	(11,10,9,14)
$R_{13} =$ < (HCH)	(6,5,7)	$R_{30} =$ CH opb	(9,8,5,11)
$R_{14} =$ < (CCH)	(9,5,6)	$R_{31} =$ C-C(R) tor	(4,5)
$R_{15} =$ < (CCH)	(9,5,7)	$R_{32} =$ C-C(T) tor	(5,9)
$R_{16} =$ < (CCC)	(4,5,9)	$R_{33} =$ C=C tor	(9,11)
$R_{17} =$ < (CCH)	(5,9,8)	$R_{34} =$ C-C(T) tor	(11,14)

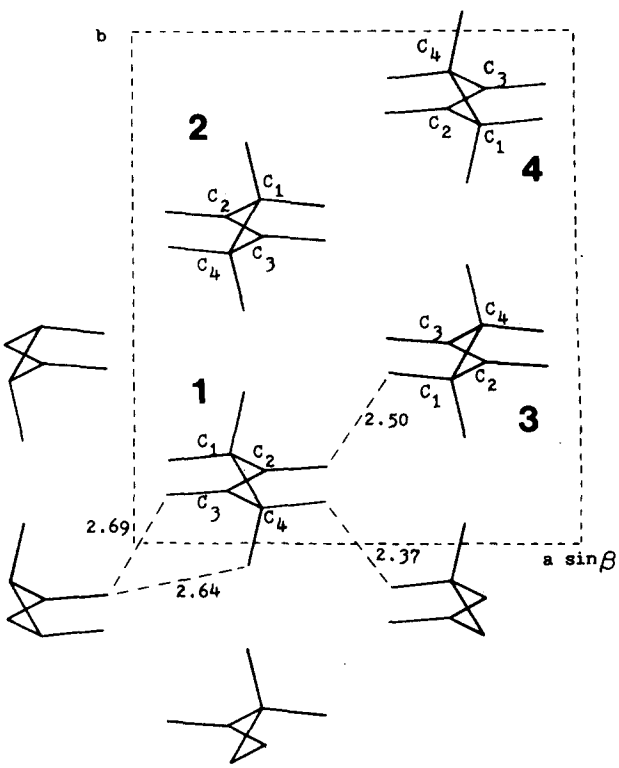

FIG. 8. Crystal structure of TPBD, projected along the *c* axis. Short H • • • H contact distances are given.

as-polymerized TPBD is not to be associated with the main crystalline chain conformation, a conclusion which will be seen to be consistent with the normal vibration calculations.

The effects of interchain interactions in the crystal are twofold: the splitting of intrachain vibrations and the appearance of lattice modes. Such splittings have been noted in the 1450-cm^{-1} region of the infrared spectrum,[8,12] and we have, in addition, observed a splitting of the band near 770 cm^{-1}. In the Raman spectra similar splittings occur, particularly at low temperatures (see Fig. 2), in the bands near 1435, 760, and 240 cm^{-1}. As we shall see, these are all consistent with the predictions from normal vibrational calculations.

The bands we have observed below 200 cm^{-1} in the infrared and Raman spectra are all assignable to lattice modes. This is indicated not only by the fact that the single-chain calculation (cf. Table IV) predicts no mode modes below 200 cm^{-1}, but by the temperature behavior of these bands. Thus, if we lower the temperature of the sample the four Raman bands exhibit large shifts to higher frequencies, as shown in Fig. 9. This is a characteristic feature of interchain modes, since the intermolecular interactions increase in magnitude as the distances diminish in the contracted unit cell. Splittings should also increase under these circumstances, and this is seen for the bands near 760 and 240 cm^{-1}. Similar effects have been noted in polyethylene.[17,18] In addition, if the TPBD sample is heated beyond the crystal phase transition these four Raman bands disappear. This is to be expected, since not only do the distances between chains increase but there is an increase in torsional oscillations within the chain,[3] both of which will have the effect of diminishing the magnitude and specificity of interchain interactions. These characteristics make for an unambiguous association of these bands with lattice modes, although the

TABLE IV. Calculated normal vibrations of a single chain of trans-1,4-polybutadiene.

Structure[a]			Assignment and potential-energy distribution[b]
B	*C*	*D*	
3026	3026	3026	Ag: CH str (98,98,98)
3009	3009	3009	Au: CH str (100,100,100)
2922	2923	2923	Ag: CH_2 asy str (98, 98, 98)
2914	2914	2914	Au: CH_2 asy str (100,100,100)
2848	2848	2848	Ag: CH_2 sym str (100,100,100)
2842	2842	2842	Au: CH_2 sym str (100,100,100)
1665	1666	1665	Ag: C=C str (76,75,75), CH ipb (16,16,16), C-C(*T*) str (14,14,16)
1436	1436	1436	Ag: CH_2 bend (98, 98, 98)
1428	1429	1432	Au: CH_2 bend (104,102,102)
1327	1324	1322	Ag: CH_2 wag (42,44,38), CH_2 twist (18,18,20), CH ipb (14,14,16)
1301	1300	1299	Ag: CH_2 twist (57,58,56), CH_2 wag (19,16,16), CH ipb (4,10,12)
1298	1296	1286	Au: CH ipb (36,38,44), CH_2 twist (28,32,44), CH_2 wag (22,14,0)
1257	1257	1260	Ag: CH ipb (36,36,32), CH_2 wag (34,36,42), C=C str (10,10,9)
1241	1244	1245	Au: CH_2 wag (76,82,100), CH_2 twist (16,10,0)
1139	1138	1136	Ag: C-C(*T*) str (30,28,24), CH_2 rock (24,26,30), CCC′ def (22,10,20)
1062	1061	1059	Au: CH_2 twist (48,46,42), CH ipb (42,38,30), C-C(*T*) str (34,38,48)
1033	1032	1026	Ag: C-C(*R*) str (79,83,79), CCC def (12,14,18)
1032	1031	1028	Au: C-C(*T*) str (62,56,48), CH ipb (22,24,30), CH_2 twist (14,18,22)
975	975	976	Au: C=C tor (62,61,61), CH opb (34,33,34)
960	944	898	Ag: CH_2 rock (38,36,34), C-C(*T*) str (14,14,18), CH opb (12,12,9), CCC def (10,12,18)
774	773	772	Au: CH_2 rock (94, 94, 92)
748	756	775	Ag: CH opb (70,66,58), CH_2 rock (12,12,6), C-C(*R*) str (4,6,14)
547	561	598	Ag: CCC′ def (44,42,34), CCC def (36,34,28), CH opb (8,10,18)
423	419	416	Au: CCC def (64,68,70), CCC′ def (20,10,3), CH opb (14,18,20), C=C tor (10,13,15)
296	303	307	Au: CCC′ def (68,84,96), C-C(*R*) tor (16,16,15)
224	234	243	Ag: C-C(*T*) tor (60,56,56), C-C(*T*) str (12,14,13), CCC def (10,10,12)

[a] See Table I for structural parameters.
[b] Numbers in parenthesis refer to structures *B*, *C*, and *D*, respectively.

TABLE V. Raman active modes of crystalline trans-1, 4-polybutadiene.

Frequency				Assignment and potential-energy distribution[a]
Observed		Calculated		
110°K	RT	A_g	B_g	
3002	2999	3030	3030	CH str (98, 98)
			3013	CH str (99)
		3012		CH str (99)
2948	2948			
2922				
2920	2920	2926	2926	CH_2 asy str (100, 99) plus combinations
2899	2900		2917	CH_2 asy str (99) and overtones
2883	2880	2916		CH_2 asy str (99)
2869				
2838	2841	2852		CH_2 sym str (98)
			2851	CH_2 sym str (98)
		2845	2845	CH_2 sym str (99, 99)
1665	1665	1665	1665	C=C str (75, 75), CH ipb (16, 16), C-C(T) str (14, 14)
1456	1456		1448	CH_2 bend (96)
1436	1436	1447		CH_2 bend (97)
1433		1434		CH_2 bend (102)
1427	1427		1434	CH_2 bend (92)
			1331	CH_2 wag (41), CH_2 twist (21), CH ipb (15)
1329	1331	1330		CH_2 wag (34), CH_2 twist (21), CH ipb (15)
			1320	CH_2 twist (51), CH_2 wag (26), CH ipb (10)
1307	1310	1318		CH_2 twist (35), CH_2 wag (26), CH ipb (10)
		1305		CH ipb (33), CH_2 twist (31), CH_2 wag (17)
			1303	CH_2 twist (34), CH ipb (32), CH_2 wag (19)
1268	1269	1265		CH_2 wag (36), CH ipb (36), C-C(T) str (12)
			1263	CH_2 wag (38), CH ipb (35), C-C(T) str (11)
		1245	1245	CH_2 wag (73, 73), CH_2 twist (15, 14)
1151	1153	1143	1143	C-C(T) str (29, 30), CH_2 rock (24, 24), CCC′ def (22, 22)
			1073	CH ipb (47), CH_2 twist (30), CH_2 bend (26), C-C(T) str (22)
		1070		CH ipb (47), CH_2 twist (29), CH_2 bend (24), C-C(T) str (23)
1014	1016	1037	1037	C-C(R) str (66, 76), C-C(T) str (17, 17)
			1035	C-C(T) str (71), CH ipb (11)
		1034		C-C(T) str (56), C-C(R) str (14), CH ipb (14)
997		988		C=C tor (60), CH opb (32)
			982	C=C tor (61), CH opb (33)
			965	CH_2 rock (37), C-C(T) str (14), CCC def (12), CH opb (11)
965	967	964		CH_2 rock (38), C-C(T) str (14), CCC def (12), CH opb (11)
		796		CH_2 rock (89)
			792	CH_2 rock (88)
764	766		758	CH opb (68), CH_2 rock (13)
759		755		CH opb (69), CH_2 rock (12)
539				noncrystalline
528	530	550	550	CCC′ def (43, 44), CCC def (36, 36), CH opb (8, 12)
		434		CCC def (61), CCC′ def (20), CH opb (12)
			431	CCC def (62), CCC′ def (20), CH opb (12)
		306		CCC′ def (63), C-C(R) tor (15), CH opb (14)
			304	CCC′ def (64), C-C(R) tor (15), CH opb (14)
251	239		243	C-C(T) tor (48), C-C(T) str (12)
237	234	239		C-C(T) tor (51), C-C(T) str (12)
145	118		127	R: $H_{1,8}H_{3,7}$(12), $H_{1,8}H_{3,10}$(11), $H_{1,8}H_{4,13}$(13)$H_{1,13}H_{4,13}$(21)
124	104	108		R: $H_{1,8}H_{4,13}$(19), $H_{1,13}H_{4,13}$(33), $H_{1,10}H_{4,10}$(10)
			88	T: $H_{1,13}H_{4,13}$(10), $H_{1,10}H_{4,12}$(13)
93	70	68		T: $H_{1,10}H_{4,12}$(19)
		59		T: $H_{1,10}H_{4,10}$(22), $H_{1,10}H_{4,12}$(12)
			58	T: $C_{1,9}H_{2,12}$(14), $H_{1,10}H_{4,10}$(26)
56	48		45	T: $H_{1,6}H_{3,7}$(10), $H_{1,8}H_{3,7}$(18), $H_{1,13}H_{4,13}$(14)
		36		T: $H_{1,6}H_{2,12}$(12), $H_{1,8}H_{4,13}$(21), $H_{1,13}H_{4,13}$(11)

[a] R—rotatory lattice mode, T—translatory lattice mode. Interacting chains (first subscript, see Fig. 8) and atoms (second subscript, see Fig. 7) are given. For these modes, there is essentially no contribution to the PED from intrachain coordinates.

specific assignments have to be determined from the normal vibration calculations.

Assignments

The specific assignments of calculated normal vibrations to observed bands will now be considered. In making these we have been guided by several general considerations: (i) the single-chain calculation was used as a preliminary indication of which unit cell modes should be strong in the infrared and which strong in the Raman spectra; (ii) the observed infrared dichroism of the bands[12] imposed the restriction that A_u modes could

TABLE VI. Infrared active modes of crystalline trans-1, 4-polybutadiene.

Frequency			Assignment and Potential Energy Distribution
Observed	Calculated		
	A_u	B_u	
3030		3030	CH (98)
	3029		CH (98)
2995	3012	3012	CH (100, 100)
2957	2925		CH_2 asy str (98)
2928		2924	CH_2 asy str (98) plus combinations
2922	2916	2916	CH_2 asy str (100, 100) and overtones
2905	2850	2850	CH_2 sym str (99, 99)
2844	2844	2844	CH_2 sym str (99, 99)
	1665	1665	C=C str (76, 75), Ch ipb (16, 16), C-C(T) str (14, 14)
1456	1442		CH_2 bend (97)
1447		1440	CH_2 bend (97)
1438	1433	1433	CH_2 bend (102, 103)
1350			noncrystalline
		1329	CH_2 wag (38), CH_2 twist (21), CH ipb (15)
1336	1328		CH_2 wag (45), CH_2 twist (14), CH ipb (17)
	1306		CH_2 twist (60), CH_2 wag (14)
1312		1304	CH_2 twist (44), CH_2 wag (25), CH ipb (15)
		1302	CH_2 twist (37), CH ipb (30), CH_2 wag (17)
	1300		CH ipb (36), CH_2 wag (22), CH_2 twist (29)
		1261	CH ipb (36), CH_2 wag (34), C=C str (10), C-C(T) str (10)
	1259		CH_2 wag (37), CH ipb (34), C=C str (10), C-C(T) str (12)
	1244		CH_2 wag (75), CH_2 twist (15)
1235		1242	CH_2 wag (76), CH_2 twist (16)
1124	1141	1141	C-C(T) str (28, 30), CH_2 rock (24, 24), CCC′ def (22, 22)
	1067		CH_2 twist (52), CH ipb (46), C-C(T) str (27)
1075			noncrystalline
		1064	CH_2 twist (48), CH ipb (42), C-C str (32)
		1035	C-C(R) str (66), C-C(T) str (12)
	1035		C-C(T) str (63), CH ipb (14), CH_2 twist (10)
	1034		C-C(R) str (72), CCC def (11)
1053		1033	C-C(T) str (52), CH_2 twist (12), CH ipb (17)
982			noncrystalline
970		985	C=C tor (60), CH opb (32)
963	979		C=C tor (61), CH opb (34)
		963	CH_2 rock (38), C-C(T) str (14), CH opb (11), CCC def (10)
	962		CH_2 rock (38), C-C(T) str (14), CH opb (11), CCC def (10)
773		785	CH_2 rock (91)
768	781		CH_2 rock (92)
	756		CH opb (68)
		754	CH opb (69)
		551	CCC′ def (42), CCC def (35)
	550		CCC′ def (43), CCC def (36)
443		427	CCC def (63), CCC′ def (20), CH opb (12)
	426		CCC def (63), CCC′ def (20), CH opb (13)
330	306		CCC′ def (66), C-C(R) str (15), CH opb (13)
		305	CCC′ def (63), C-C(R) tor (15), CH opb (14)
	240		C-C(T) tor (49), C-C(T) str (12)
		233	C-C(T) tor (54), C-C(T) str (12)
104	102		T: $H_{1,3}H_{3,7}(11)$, $H_{1,8}H_{3,7}(22)$, $H_{1,8}H_{3,10}(17)$, $H_{1,10}H_{4,12}(12)$
64		76	T: $H_{1,3}H_{3,6}(13)$, $H_{1,6}H_{3,7}(10)$, $H_{1,8}H_{4,12}(18)$, $H_{1,10}H_{4,12}(20)$
		58	R: $C_{1,9}H_{2,12}(15)$, $H_{1,8}H_{3,7}(16)$, $H_{1,8}H_{3,10}(13)$
	54		R: $H_{1,8}C_{3,5}(10)$, $H_{1,6}H_{3,7}(25)$
	35		T: $H_{1,6}H_{2,12}(15)$, $H_{1,8}H_{3,7}(25)$

not be assigned to bands polarized parallel to the chain axis (B_u modes can have parallel or perpendicular dichroism); and (iii) in general, strong Raman bands were assigned to the A_g components of the unit-cell modes.

In the C-H stretching region, the bands are moderately well assigned to the predicted modes. The main problem, particularly in the Raman spectrum, is the presence of more observed bands than calculated modes. It must be realized, however, that overtones and combinations are Raman active and can contribute in this region. For example, $2\times1436\ (A_g)=2872\ (A_g)$; $2\times1456\ (A_u)=2912\ (A_g)$; $2\times1447\ (A_u)=2894\ (A_g)$; and $1665\ (A_g)+1268\ (A_g)=2933\ (A_g)$. It is, therefore, difficult to be more definitive about these assignments at the present time.

In the CH_2 bending region there is an adequate accounting of the predicted modes, although the frequency ordering between infrared and Raman could be improved. This may be due to residual inadequacies in the intrachain potential function.[4]

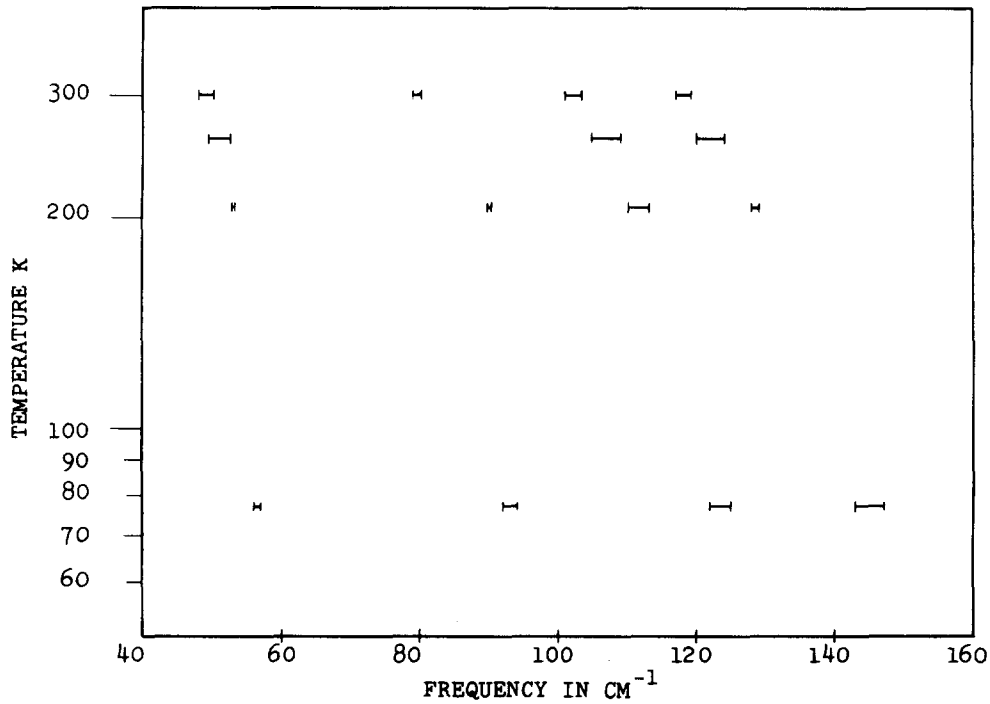

FIG. 9. Effect of temperature on the positions of the low-frequency Raman bands.

The CH_2 wagging and twisting modes are well assigned in both Raman and infrared. In the former case the ratio of I(1331)/I(1310) increases significantly between the room-temperature and low-temperature spectra, from 2.0 to 2.4. We associate this change, which is reversible, with a more-perfect chain order at the lower temperature.

Observed bands in the C-C stretching region agree fairly well with those calculated. The same is true for the C=C stretch, CH out-of-plane bend modes in the infrared near 970 cm^{-1}. In fact, both the interaction splitting as well as the dichroisms are predicted by the calculation. This suggests that the shoulder observed at about 982 cm^{-1} should be assigned to a noncrystalline structure.

Interchain interactions account well for the splitting in the infrared active CH_2 rocking mode near 770 cm^{-1}, which is observed in all of our samples. (Preliminary results indicate that this splitting is enhanced at low temperature, as expected.) The same is true for the Raman active CH out-of-plane bend, CH_2 rock near 760 cm^{-1}, although the splitting is only manifested clearly in the low temperature spectrum.

The C=C-C deformation mode is calculated at 550 cm^{-1} in the Raman spectrum and is not predicted to be split by interchain interactions (which is not unreasonable since the mode involves very little H motion, and it is H motions which are most strongly affected by the H···H interchain interactions). This fact suggests that the shoulder observed at 539 cm^{-1} is not to be assigned to a crystalline chain conformation, which, as we noted earlier, is also consistent with the results on single crystals.

The C-C torsion modes are reasonably well reproduced, as is the splitting (234 and 239 cm^{-1}) predicted in the Raman spectrum. The significant increase in this splitting observed at low temperature (237 and 251 cm^{-1}) confirms the interchain origin of this effect.

The lattice modes are reasonably well assigned on the basis of the calculated frequencies, although some uncertainties may still exist. We plan to obtain low-temperature infrared spectra, as well as spectra below 30 cm^{-1}, which should assist in strengthening these assignments. As will be seen from Tables V and VI, the H···H interactions predominate in determining these low-frequency modes.

CONCLUSIONS

The addition of interchain atom-atom potentials to the intrachain force field of TPBD is seen to account satisfactorily for the band splittings and low-frequency lattice modes observed in the infrared and Raman spectra of this polymer. The analysis of the vibrational spectrum is significantly aided by our having spectra of a polymer prepared in urea complex, since this polymer contains essentially 100% trans units. Investigation of the as-polymerized polymer as well as single crystals grown from solution permits a distinction to be made between bands associated with crystalline and noncrystalline conformations.

This initial satisfactory analysis of the vibrational spectrum of crystalline TPBD should permit a study of chain fold morphology in single crystals of TPBD by mixed-crystal methods similar to those used for polyethylene.[19] We hope to undertake such a study. It should also make possible a more reasonable refinement of the intrachain potential function. Our analysis has already elucidated spectral changes associated with the crystal-crystal phase transition,[3] on which we will report subsequently.[20]

ACKNOWLEDGMENT

The authors are indebted to C. E. Wilkes of the B. F. Goodrich Company for providing us with the urea-complex TPBD. We wish to thank J. F. Rabolt for help in obtaining the far-infrared spectra, and K. Shaw for help in obtaining some of the Raman spectra. One of us (S. L. H.) wishes to thank the Macromolecular Research Center for fellowship support. This research was also supported by National Science Foundation Grant No. GP-38093.

[1]G. Natta and P. Corradini, Nuovo Cimento Suppl. **1**, 9 (1960).
[2]S. Iwayanagi, I. Sakurai, T. Sakurai, and T. Seto, J. Macromol. Sci. Phys. **2**, 163 (1968).
39 (1970).
[4]N. Neto and C. di Lauro, Eur. Polym. J. **3**, 645 (1967).
[5]S. W. Cornell and J. L. Koenig, Macromolecules **2**, 540 (1969).
[6]C. Hendrix, D. A. Whiting, and A. E. Woodward, Macromolecules **4**, 571 (1971).
[7]J. J. White, A. U. Hasan, and W. C. Sears, J. Macromol. Sci. Phys. **7**, 177 (1973).
[8]T. Oyama, K. Shiokawa, and Y. Murata, Polymer J. **6**, 549 (1974).
[9]D. M. White, J. Am. Chem. Soc. **82**, 5678 (1960).
[10]Y. Chatani and S. Kuwata, Macromolecules **8**, 12 (1975).
[11]J. M. Stellman and A. E. Woodward, J. Polymer Sci. A-2, **9**, 59 (1971).
[12]D. Morero, J. Ciampelli, and E. Mantica, *Advances in Molecules Spectroscopy*, edited by A. Mangini (Pergamon, Oxford, 1962), Vol. 2, p. 898.
[13]D. E. Williams, J. Chem. Phys. **45**, 3770 (1966).
[14]D. E. Williams, J. Chem. Phys. **43**, 4424 (1965).
[15]J. M. Stellman, A. E. Woodward, and S. D. Stellman, Macromolecules **6**, 330 (1973).
[16]T. Tatsumi, T. Fukushima, K. Imada, and M. Takayanagi, J. Macromol. Sci. Phys. **1**, 459 (1967).
[17]M. Tasumi and S. Krimm, J. Chem. Phys. **46**, 755 (1967).
[18]M. I. Bank and S. Krimm, J. Appl. Phys. **39**, 4951 (1968).
[19]S. Krimm, *Proceedings of the International Symposium on Macromolecules*, Rio de Janeiro (Elsevier Publishing Co., New York, 1974), p. 107.
[20]S. L. Hsu and S. Krimm (unpublished).